

# Polarization in microlensing towards the Galactic bulge

G. Ingrosso,<sup>1,2\*</sup> S. Calchi Novati,<sup>3,4</sup> F. De Paolis,<sup>1,2</sup>  
Ph. Jetzer,<sup>5</sup> A. A. Nucita,<sup>1,2</sup> F. Strafella<sup>1</sup> and A. F. Zakharov<sup>6,7</sup>

<sup>1</sup> *Dipartimento di Matematica e Fisica, “Ennio De Giorgi”, Università del Salento, CP 193, I-73100 Lecce, Italy*

<sup>2</sup> *INFN Sezione di Lecce, CP 193, I-73100 Lecce, Italy*

<sup>3</sup> *Dipartimento di Fisica “E. R. Caianiello”, Università di Salerno, Via Ponte don Melillo, 84084 Fisciano (SA), Italy*

<sup>4</sup> *Istituto Internazionale per gli Alti Studi Scientifici (IIASS), Vietri Sul Mare (SA), Italy*

<sup>5</sup> *Institute for Theoretical Physics, University of Zürich, Winterthurerstrasse 190, CH-8057 Zürich, Switzerland*

<sup>6</sup> *Institute of Theoretical and Experimental Physics, B. Chermushkinskaya 25, 117259 Moscow, Russia*

<sup>7</sup> *Bogoliubov Laboratory of Theoretical Physics, Joint Institute for Nuclear Research, 141980 Dubna, Russia*

Accepted xxx; Received xxx; in original form xxx

## ABSTRACT

Gravitational microlensing, when finite size source effects are relevant, provides an unique tool for the study of source star stellar atmospheres through an enhancement of a characteristic polarization signal. This is due to the differential magnification induced during the crossing of the source star. In this paper we consider a specific set of reported highly magnified, both single and binary exoplanetary systems, microlensing events towards the Galactic bulge and evaluate the expected polarization signal. To this purpose, we consider several polarization models which apply to different types of source stars: hot, late type main sequence and cool giants. As a result we compute the polarization signal  $P$ , which goes up to  $P=0.04$  percent for late type stars and up to a few percent for cool giants, depending on the underlying physical polarization processes and atmosphere model parameters. Given a  $I$  band magnitude at maximum magnification of about 12, and a typical duration of the polarization signal up to 1 day, we conclude that the currently available technology, in particular the polarimeter in FORS2 on the VLT, potentially may allow the detection of such signals. This observational programme may take advantage of the currently available surveys plus follow up strategy already routinely used for microlensing monitoring towards the Galactic bulge (aimed at the detection of exoplanets). In particular, this allows one to predict in advance for which events and at which exact time the observing resources may be focused to make intensive polarization measurements.

**Key words:** Gravitational Lensing - Physical data and processes: polarization - The Galaxy: bulge

## 1 INTRODUCTION

Gravitational microlensing, initially developed to search for MACHOs in the Galactic halo and near the Galactic disc (Paczynski 1986; Alcock et al. 1993; Aubourg et al. 1993; Udalski et al. 1993, 1994) has become nowadays a powerful tool to investigate several aspects of stellar astrophysics and also to search for extrasolar planets orbiting around lens stars.

Indeed, microlensing gives the opportunity to study the star’s limb-darkening profile, which is the variation of the intensity from the disc center to the limb, and thus to test

stellar atmosphere models. At the same time, microlensing leads to the discovery and the detailed characterization of exoplanetary systems when planetary deviations in the light-curves expected for single-lens events are detected (see Dominik (2010) and Gaudi (2010) for recent reviews).

Microlenses can spatially resolve a source star thanks to caustic structures created by a lens system (Schneider, Ehlers & Falco 1992). Caustics are formed by a set of closed curves, along which the point source magnification is formally infinite, with a steep increase in magnification in their vicinity. This increase is so steep that the characteristic length scale of the differential magnification effect is of the order of a fraction of the source star radius. In this way different parts of the source star are magnified by substantially different amounts. The resulting lensing light-

\* E-mail: ingrosso@le.infn.it

curve deviates from the standard form expected for a point source event (Witt & Mao 1994; Gould 1994; Alcock et al. 1997) and the analysis of the deviations enables to measure the limb-darkening profile of the lensed star.

Early works (Witt & Mao 1995; Loeb & Sasselov 1995; Valls-Gabaud 1998; Heyrovský 2003) have pointed out the sensitivity of microlensing light-curves to limb-darkening, with the aim to help to remove the microlensing model parameter degeneracy. The specific use of microlensing as a tool to study stellar atmospheres was proposed later (Hendry et al. 1998; Gaudi & Gould 1999), in particular to probe atmospheres of red giants in the Galactic bulge (Heyrovský & Sasselov 2000).

The best candidate events for studying stellar atmospheres are highly magnified microlensing events, which also show relevant finite size source effects. For these events the lens and the background source star are almost aligned and the lens passes over the surface of the source star (*transit* events). Although relatively rare, these events potentially contain unique information on the stellar atmosphere properties of the source star as shown by Fouqu e et al. (2010) and Zub et al. (2010). Indeed, besides the brightness profile of a remote source star disc, highly magnified events with large finite size source effects allow to measure the lens Einstein radius  $R_E$  (if the physical radius  $R_*$  of the source is known) and provide a unique chance to study spectroscopically Galactic bulge stars.

The light-curve analysis of highly magnified events is also sensitive to the presence of lens planetary companions, in particular when the planet-to star distance is of the order of  $R_E$ . The same opportunity for studying stellar atmospheres is offered by binary microlensing due to caustic crossing as the source passes through fold (Schneider, Ehlers & Falco 1992) and cusp caustics (Schneider & Weiss 1992; Zakharov 1995).

The aim of the present paper is to consider polarization variability of the source star light for real events, taking into account different polarization mechanisms according to the source star type. Indeed, variations in the polarization curves are similar to finite source effects in microlensing when color effects may appear due to limb darkening and color distribution across the disc (Witt & Mao 1994; Bogdanov & Cherepashchuk 1995a,b; Gaudi & Gould 1999; Bogdanov & Cherepashchuk 2000, 2002; Dominik 2005; Heyrovský 2007).

It is known that the light received from the stellar limb may be significantly (up to about 12 percent) polarized due to the so called Sobolev – Chandrasekhar effect (Sobolev 1949; Chandrasekhar 1960; Sobolev 1963). Polarization parallel to the limb of the source is caused by photon (Thomson) scattering off free electrons, when the light passes through the stellar atmosphere. This polarization mechanism is effective for hot stars of any luminosity class which, indeed, have a free electron atmosphere.

It is also known that, by a minor extent, the continuum spectrum of the main sequence stars of late type is linearly polarized by coherent (Rayleigh) scattering on neutral hydrogen in its ground state and, with a minor contribution, by scattering on free electrons (Fluri & Stenflo 1999). The polarization in late type stars has been measured only for the Sun (for which due to the distance the projected disc is spatially resolved) and also in this case as for hot stars,

the polarization gets its maximum value near the solar limb, due to the most favorable geometry there.

However, the light received from the stars is usually unpolarized, since the flux from each stellar disc element is the same. A net polarization of the stellar light may be introduced by some suitable asymmetry in the stellar disc (e.g. eclipses, tidal distortions, stellar spots, fast rotation, magnetic fields) and also in the propagation through the interstellar medium (Bochkarev, Karitskaya & Sakhbulin 1985; Dolginov, Gnedin & Silant'ev 1995).

In the microlensing context, polarization in the stellar light is induced due to the proper motion of the lens star through the source star disc, during which different parts are magnified by different amounts. Therefore, the gravitational lens scans the disc of the background star giving rise not only to a time dependent gravitational magnification of the source star light but also to a time dependent polarization.

As for the limb-darkening brightness profile, the polarization degree is maximized when the source trajectory crosses regions with high magnification gradient. This occurs in *transit* events since the magnification of the source star flux increases as the lens approaches closer to the source star, and during binary microlensing events since now there is the opportunity for caustic crossing.

Accordingly, we consider the polarization variability for the *transit* events (with lenses passing over source stars) selected by Choi et al. (2011) and for a subset of exoplanetary events towards the Galactic bulge (Gaudi 2010). Exoplanetary events are binary lens systems characterized by values of the planet-to-star mass ratio  $q \ll 1$  and have smaller star-to-planet distance  $d$  as compared to the separation of the stars in a binary system. A full treatment of the polarization in binary microlensing events will be the subject of a subsequent paper. Here, selecting a representative sample of exoplanetary events, we show how the polarization works in binary microlensing.

The idea that polarization induced by an electron scattering atmosphere could be enhanced by gravitational microlensing and eventually observed was first raised and investigated in relation to supernovae by Schneider & Wagoner (1987). In particular, the observation of a variable polarization due to a supernova beam expanding in a self-gravitating system constituted by individual masses ( $\gtrsim 10^{-3} M_\odot$ ) may indicate the presence of dark matter objects.

Then, Simmons, Newsam & Willis (1995a), Simmons, Willis & Newsam (1995b) and Bogdanov, Cherepashchuk & Sazhin (1996) pointed out that the polarization of star light induced by an electron scattering atmosphere is enhanced by the microlensing effect and that the relative motion of source and lens causes a time variation of the source polarization degree. Simmons, Newsam & Willis (1995a) and Simmons, Willis & Newsam (1995b) also present a numerical calculation of the polarization degree induced by a single-lens (the Schwarzschild lens), showing that during a microlensing event the polarization profile has a double peak for *transit* events, (where a part of the source disc is aligned with the lens and observer), while it has a single peak in the *bypass* events (where the source trajectory remains outside the lens).

Assuming that the source star has an electron scatter-

ing atmosphere, Agol (1996) calculated the time-dependent polarization of a star being gravitationally lensed by a binary system. Polarization as high as  $P \simeq 1$  percent can be achieved if the star crosses a caustic or passes near a cusp; otherwise, the maximum polarization is  $\simeq 0.1$  percent.

Polarization by non-compact microlenses (Gurevich & Zybin 1995; Zakharov & Sazhin 1996a,b; Zakharov 1999, 2010) was also analyzed (Belokurov & Sazhin 1998; Zakharov 1998) since a source may cross caustics arising in the model.

The most likely candidates for observing polarization variability during microlensing events would be young, hot giant star sources, because they have electron scattering atmospheres needed for producing limb polarization through Thomson scattering (Simmons, Willis & Newsam 1995b). Unfortunately, the bulge of the Galaxy does not contain a large number of hot giant stars. However, polarization may be also induced by the scattering of star light off atoms, molecules and dust grains in the adsorptive atmospheres of evolved, cool stars as shown by Simmons et al. (2002) and Ignace, Bjorkman & Bryce (2006). These more ubiquitous stars, that do not have levels of polarization as high as those predicted by the Chandrasekar model, may display an intrinsic polarization of up to several percent, due to the presence of stellar winds that give rise to extended adsorptive envelopes. This is the case for many cool giant stars, in particular for the red giants. Such evolved stars constitute a significant fraction of the lensed sources towards the Galactic bulge, the LMC (Alcock et al. 1997) and the M31 galaxy (Calchi Novati 2010), making them valuable candidates for observing variable polarization during microlensing events.

Polarization measurements on ongoing microlensing events can be useful for further characterizing them, for testing stellar atmosphere models and to complement finite source measurements (Gould 1994). In this respect, the detection of a variable polarization leads to an independent measure of the angular Einstein radius  $R_E$  of the lens, the position angle of the lens and the velocity direction in the sky (Yoshida 2006).

Of course, since accurate polarization measurements cannot be obtained with a survey telescope, alert systems are necessary allowing other larger telescopes to take polarimetric measurements during a microlensing event.

For definiteness, we consider the observed sample of highly magnified, single-lens *transit* events (Choi et al. 2011) and a subset of exoplanetary events observed towards the Galactic bulge (Gaudi 2010). For these events we calculate the polarization profiles as a function of time taking into account the nature of the source stars. As an illustration, we also consider the expected polarization signal for the PA-99-N2 event towards M31 (Paulin-Henriksson et al. 2003).

## 2 POLARIZATION MODELS

### 2.1 Basic equations

Let us consider the linear polarization of light scattered in a stellar atmosphere. Following the approach in Chandrasekhar (1960) we define the intensities  $I_l(\mu)$  and  $I_r(\mu)$  emitted by the scattering atmosphere in the direction making an angle  $\chi$  with the normal to the star surface and

polarized as follows:  $I_l(\mu)$  is the intensity in the plane containing the line of sight and the normal,  $I_r(\mu)$  is the intensity in the direction perpendicular to this plane (light propagates in the direction  $\mathbf{r} \times \mathbf{l}$ ). Here  $\mu = \cos \theta$  and we are assuming that the polarization is a function only of  $\mu$ . The center-to-limb variation in the polarization across the stellar disc originates from the contribution of the scattering opacity to the total opacity in the star atmosphere. The polarization typically increases from the center ( $\mu = 1$ ) to the stellar limb ( $\mu = 0$ ) since we tend to see more scattered, hence polarized, light towards the limb. In the hot stars, electron (Thomson) scattering is one cause of opacity. In the case of cool stars, coherent (Rayleigh) scattering on atomic and molecular hydrogen and atomic helium, and scattering off dust grains provide the main source of the scattering opacity.

We choose a coordinate system in the lens plane with the origin at the center  $(x_0, y_0)$  of the projected position of the source star. The  $Oz$  axis is directed towards the observer, the  $Ox$  axis is directed towards the lens (in single-lens events) and oriented parallel to the star-to-planet separation (in binary events). The location of a point  $(x, y)$  on the star surface is determined by the angular distance  $\rho$  from the origin of the coordinates and by the angle  $\varphi$  with the  $Ox$  axis ( $x = x_0 + \rho \cos \varphi$  and  $y = y_0 + \rho \sin \varphi$ ). In the above coordinate system  $\mu = \sqrt{1 - \rho^2/R^2}$ , where  $R$  is the star angular size. Here and in the following all distances are given in units of the Einstein radius  $R_E$  of the total lens mass.

To calculate the polarization of a star with center at the position  $(x_0, y_0)$  we integrate the unnormalized Stokes parameters and the flux over the star (Simmons, Newsam & Willis 1995a; Simmons, Willis & Newsam 1995b; Agol 1996)

$$F = F_0 \int_0^{2\pi} \int_0^R A(x, y) I_+(\mu) \rho d\rho d\varphi, \quad (1)$$

$$F_Q = F_0 \int_0^{2\pi} \int_0^R A(x, y) I_-(\mu) \cos 2\varphi \rho d\rho d\varphi, \quad (2)$$

$$F_U = F_0 \int_0^{2\pi} \int_0^R A(x, y) I_-(\mu) \sin 2\varphi \rho d\rho d\varphi, \quad (3)$$

where  $F_0$  is the unamplified star flux,  $A(x, y)$  the point source amplification due to the lens system and

$$I_+(\mu) = I_r(\mu) + I_l(\mu), \quad (4)$$

$$I_-(\mu) = I_r(\mu) - I_l(\mu). \quad (5)$$

As usual, the polarization degree and the polarization angle are (Chandrasekhar 1960)

$$P = \frac{\sqrt{F_Q^2 + F_U^2}}{F}, \quad \theta_P = \frac{1}{2} \tan^{-1} \frac{F_U}{F_Q}. \quad (6)$$

Clearly, neglecting other distorting factors, the stellar light will be unpolarized if we observe the source star without any gravitational lens effect since, due to the symmetry of their expressions, the parameters  $F_Q$  and  $F_U$  are equal to zero. The gravitational field produced by the lensing system breaks the spherical symmetry over the projected stellar disc and thus results in a non-vanishing polarization.

For single-lens events the amplification is (Einstein

1936; Paczyński 1986)

$$A(x, y) = \frac{\rho_s + 2}{\rho_s \sqrt{\rho_s^2 + 4}}, \quad (7)$$

where

$$\rho_s^2 = \rho_0^2 + \rho^2 - 2\rho_0\rho \cos \varphi \quad (8)$$

is the angular distance between the considered surface element on the stellar disc and the lens position. Here  $\rho_0$  ( $\rho$ ) is the angular distance of the lens (the surface element) from the star center<sup>1</sup>.

In the case of binary events, we evaluate the amplification map  $A(x, y)$  at any point in the source plane by using the Inverse Ray-Shooting method (Kayser, Refsdal & Stabell 1986; Wambsganss 1997). In this case the amplification map depends on the mass ratio  $q$  between the planet and the star and the star-to-planet separation  $d$ .

The other quantities entering in the above equations are the coordinates of the source star center. These are given at any time  $t$  in terms of the other lens system parameters: the impact parameter  $u_0$  (the minimum distance of the source star center projected on the lens plane from the center of mass of the lens system), the maximum amplification time  $t_0$ , the Einstein time  $t_E$  and, for binary events, the angle  $\alpha$  that the source trajectory makes with the  $Ox$  axis.

To derive a quantitative expression of the functions  $I_l(\mu)$  and  $I_r(\mu)$  in the above equations one has to consider the relevant physical mechanism giving rise to the variable polarization degree.

## 2.2 The hot star case

In the case of polarization of stellar light induced by the electron scattering in the atmosphere of hot stars, the functions  $I_l(\mu)$  and  $I_r(\mu)$  have been evaluated (assuming a plane-parallel atmosphere) by Chandrasekhar (1960) and their numerical values can be approximated<sup>2</sup> by the following expressions (Bochkarev & Karitskaya 1983)

$$I_+(\mu) = \left( \frac{1 + 16.035\mu + 25.503\mu^2}{1 + 12.561\mu + 0.331\mu^2} \right), \quad (9)$$

$$I_-(\mu) = \left( \frac{0.1171 + 3.3207\mu + 6.1522\mu^2}{1 + 31.416\mu + 74.0112\mu^2} \right) (1 - \mu). \quad (10)$$

## 2.3 The late type main sequence star case

The continuum spectrum of the Sun is linearly polarized by coherent scattering on neutral hydrogen in its ground state (Rayleigh scattering) and, with a minor contribution, by (Thomson) scattering on free electrons<sup>3</sup>. The polarization is maximum near the solar limb due to the most fa-

vorable geometry there. Fluri & Stenflo (1999) developed a theoretical study for the formation of the continuum polarization, identifying the relevant physical mechanisms and clarifying their relative roles. The key physical quantities are the scattering coefficients and the temperature gradient in the stellar layer where polarization is formed. With a solar model atmosphere as input, the polarization is obtained by numerically solving the transfer equation for polarized radiation. The results of their numerical calculations are approximated by semi-analytical formulas, as a function of  $\mu$  and of wavelength  $\lambda$  (Stenflo 2005)

$$P(\mu) = q_\lambda \frac{(1 - \mu^2)}{(\mu + m_\lambda)(I_\lambda(\mu)/I_\lambda(1))}, \quad (11)$$

where  $I_\lambda(\mu)/I_\lambda(1)$  represents the center-to-limb variation of the intensity. The dependence of  $q_\lambda$  and  $m_\lambda$  from the wavelength is represented by the relations  $\log(q_\lambda) = a_0 + a_1\lambda + a_2\lambda^2$  and  $m_\lambda = b_0 + b_1\lambda$ , where the coefficients are determined by fitting solar observations for different wavelengths and atmosphere models (see Table 1 in Stenflo (2005)). In particular, in the I band  $q_I = 4.2 \times 10^{-4}$  and  $k_I \equiv m_I^{-1} = 50$ .

Following Carciofi & Magalhaes (2005), we adopt the model in eq. (11) for calculating the polarization profile for late type stars of any spectral type (F, G, K, M), for which polarization measurements do not exist. For the total intensity we use the linear limb-darkening profile (Choi et al. 2011)

$$I_\lambda(\mu) = \left[ 1 - \Gamma_\lambda \left( 1 - \frac{3}{2}\mu \right) \right], \quad (12)$$

where the parameter  $\Gamma_\lambda$  depends on wavelength, spectral type, surface gravity and metallicity of the source star (Claret 2000).

## 2.4 The case for cool giant stars

Polarization signals in microlensing of stars with extended circumstellar envelopes have been studied by Simmons et al. (2002) for a single-lens and in binary lensing by Ignace, Bjorkman & Bryce (2006). As emphasized in these works, the model is well suited to describe polarization in evolved, cool stars that exhibit stellar winds significantly stronger than those of the Sun. The scattering opacity responsible for producing the polarization is the photon scattering on atomic and molecular species (Rayleigh) or on dust grains.

The scattering number density distribution in the stellar envelope was parametrized by a simple power law

$$n(r) = n_h (R_h/r)^\beta, \quad (13)$$

where  $r = (\rho^2 + z^2)^{1/2}$  is the radial distance from the star center and  $n_h$  is the number density at the radius  $R_h$  of a central cavity. Indeed, since dust grains and molecules cannot form at temperatures higher than 3000 K – 4000 K, a circumstellar cavity was considered between the photosphere radius  $R$  and the condensation radius  $R_h$ , where the temperature drops to 1500 K.

The star envelope was assumed optically thin and the relevant scattering cross-section was evaluated in the dipole approximation. The relevant expressions for the Stokes parameters are given in the paper by Simmons et al. (2002),

<sup>1</sup> In the case of microlensing by a single-lens system the Stokes parameter  $F_U$  vanishes in the adopted system of coordinates defined by the line joining the lens and the star, and the polarization position angle is always perpendicular to that line.

<sup>2</sup> As noted by Bochkarev & Karitskaya (1983), the precision of the assumed approximations is better than  $10^{-3}$ .

<sup>3</sup> A polarization in spectral lines is also produced by coherent scattering in atomic bound-bound transitions.

where one can see that the polarization degree linearly depends on the optical depth  $\tau_\lambda$ . It has also been found that the polarization degree during microlensing can reach values up to a few percent, provided that  $\tau_\lambda \simeq 0.1$ .

An estimate of the order of magnitude of  $\tau_\lambda$  was also derived assuming that the gas density profile in the stellar wind follows the law

$$\rho_{\text{gas}}(r) = \frac{\dot{M}}{4\pi r^2 v(r)}, \quad (14)$$

with  $v(r) \simeq v_\infty(1 - R_h/r)^\gamma$  ( $\gamma \simeq 1/2$ ), and considering the main contribution to the gas opacity at temperature  $T < 10^3$  K. If dust grains are the main source to the stellar opacity, the optical depth is (Ignace, Bjorkman & Bunker 2008)

$$\tau_\lambda = 2 \times 10^{-3} \sigma \mathcal{K}_\lambda \left( \frac{\dot{M}}{10^{-9} M_\odot \text{yr}^{-1}} \right) \left( \frac{30 \text{ km s}^{-1}}{v_\infty} \right) \left( \frac{24 R_\odot}{R_h} \right), \quad (15)$$

where  $\sigma \simeq 0.01$  is the dust-to-gas mass density ratio and  $\mathcal{K}_\lambda \simeq 200 \text{ cm}^2 \text{ g}^{-1}$  is the dust opacity at  $\lambda > 5500 \text{ \AA}$  (Ferguson et al. 2005). This means that the wind mass-loss rate must be around  $10^{-7} M_\odot \text{ yr}^{-1}$  to obtain  $\tau_\lambda \simeq 0.1$ . This level of mass loss can be achieved only in AGB stars. This class of stars constitutes the sources of only a few of the observed microlensing events, while much more common are subgiants and red giant stars. For a realistic estimate of the polarization level for these stars, one has to relate  $\tau_\lambda$  to the stellar parameters of the magnified star. Indeed, it is well known that from main sequence to AGB phases, the mass-loss rate increases by 7 order of magnitude (Ferguson et al. 2005). By performing simulations of the mass loss of intermediate and low-mass stars, it was shown that the increase of mass loss is a continuous function (while the velocity and temperature evolutionary traces show gaps between the subgiant and AGB phases) and that  $\dot{M}$  obeys the relation (Ferguson et al. 2005)

$$\dot{M} = 2 \times 10^{-14} \frac{(L/L_\odot)(R/R_\odot)^3 (T/T_\odot)^9}{(M/M_\odot)^2} M_\odot \text{ yr}^{-1}. \quad (16)$$

So, for the more common stars evolving from main sequence to red giant star phases (see also Fig. 15 in Suzuki (2007)), mass loss rates between  $(10^{-13} - 10^{-8}) M_\odot \text{ yr}^{-1}$  are expected. This corresponds to values of  $\tau_\lambda$  in the range  $4 \times 10^{-7} - 4 \times 10^{-2}$  and, therefore, to polarization degree that are not always negligible, reaching values up to 0.5 percent.

Here, we adopt the above formalism to derive the polarization profiles for source stars with envelopes. To this aim, the Stokes parameters are numerically evaluated by using in eqs. (1), (2) and (3) the relevant expressions for  $I_+(\mu, \varphi)$  and  $I_-(\mu, \varphi)$ , as given by Ignace, Bjorkman & Bryce (2006).

### 3 POLARIZATION RESULTS

To make predictions of the polarization behavior during microlensing we have generated a large sample of single and binary lens events. Assuming the nature of the source star (a hot star, a late type main sequence or a cool giant star) and its radius  $\rho_*$ , we explore the multidimensional space for microlensing ( $u_0$ ,  $t_E$ ,  $R_E$ ) and planetary ( $q$ ,  $d$ ,  $\alpha$ ) parameters (Ingrasso et al. 2006, 2009), with the aim of deriving the polarization signal and eventually its observability. For

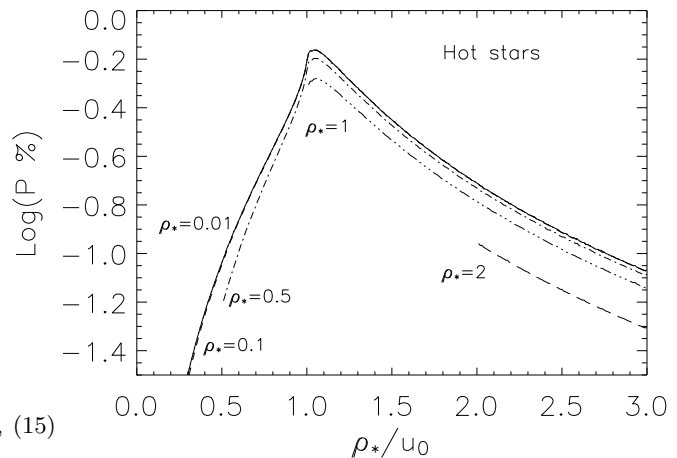


**Figure 1.** Polarization degree  $P$  in percent versus  $\rho_*/u_0$ , for different values of  $\rho_* = 0.01, 0.1, 0.5, 1, 2$  in the case of hot stars with polarization à la Chandrasekhar.

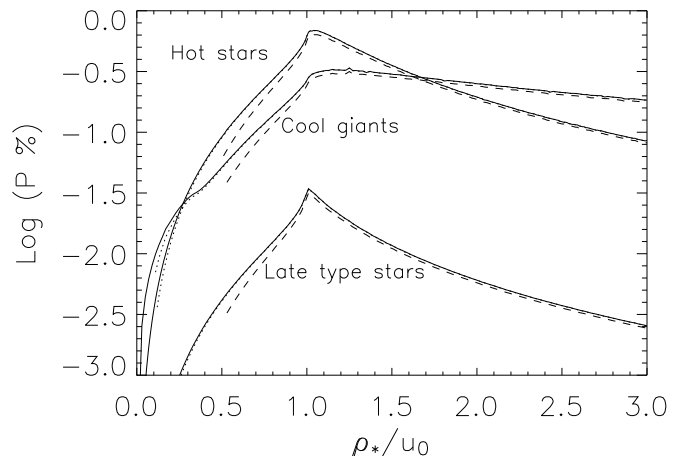


**Figure 2.** Polarization  $P$  in percent versus  $\rho_*/u_0$  and  $\rho_* = 0.01, 0.1, 0.5$  for hot stars, cool giants ( $\tau = 10^{-3}$ ,  $\beta = 2$ ,  $R_h = 5 R_*$ ) and late type stars ( $q_I = 4.2 \times 10^{-4}$ ,  $k_I = 50$ ,  $\Gamma_I = 0.5$ ).

a given set of parameters of both the source and lens system, we first evaluate the amplification map in the lens plane and then the corresponding polarization curve, which shows a continuous variation with time, depending on the source position in the lens plane.

For single-lens events, generally, the maximum polarization degree takes place at the time  $t_0$  of the maximum amplification. This happens when  $\rho_*/u_0 < 1$  (*by-pass* events) for which the source trajectory remains outside the lens. For single-lens events with  $\rho_*/u_0 > 1$  (*transit* events) for which some part of the source is directly aligned with the lens center and observer, the polarization curve has two maxima and one minimum, bracketed by the maxima, which coincides with the instant of maximum amplification (Simmons, Newsam & Willis 1995a; Simmons, Willis & Newsam 1995b). In the case of *transit* events, the polarization signal gets the maximum value when the source disk enters and exits the fold caustic (two peaks

appear at symmetrical position with respect to  $t_0$ ). In this case, the characteristic time scale  $\Delta t_*$  between the two peaks of the polarization curve is related to the *transit* duration of the source disc by (Choi et al. 2011)

$$\Delta t_* \simeq 2t_E \times \sqrt{\rho_*^2 - u_0^2}. \quad (17)$$

In binary microlensing events, for which there are a central (stellar) and one or two planetary caustics depending on the star-to-planet separation  $d > 1$  or  $d < 1$ , respectively, significant polarization may be induced when the star trajectory intersects one of the caustics. Then, a polarization peak occurring at  $t \neq t_0$  implies that a planetary caustic is intersected by the source. Moreover, as for single-lens events, if the star source *bypasses* one caustic (central or planetary), a single polarization peak appears in the polarization profile at the time of nearest approach, while a double-peak feature occurs if the stellar disc *transits* a caustic.

Therefore, detection of polarization signals may allow, in principle, to distinguish between single and binary lens events. Indeed, single and binary events can be separated by the presence of a polarization signal at  $t \neq t_0$  or by an eventual asymmetry in the polarization curve (near  $t_0$ ) induced by the planetary caustic. This happens for events with  $b \simeq 1$ , for which the planetary caustic shifts in a position close to the central one.

In general, the polarization signal in binary microlensing events depends on the projected source trajectory in the lens plane, the size and position of the caustics and the diameter of the source disc. In Section 3.2 we consider, as an example, some exoplanetary events well observed towards the Galactic center, leaving a detailed study of the polarization in binary microlensing events to a subsequent analysis.

For single-lens events and polarization induced by electron scattering in the atmosphere of hot stars, in Fig. 1 we show the polarization degree  $P$  (in percent) as a function of the ratio  $\rho_*/u_0$ . As one can see, for  $\rho_*/u_0 \gtrsim 0.3$  and  $\rho_* \lesssim 0.1$ , the polarization degree depends only on the ratio  $\rho_*/u_0$  (see also Fig. 3 in Yoshida (2006)). The polarization degree has the maximum value  $P_{\max} \simeq 0.7$  percent at  $\rho_*/u_0 \simeq 1.04$  and for low  $\rho_*$  values. For large values of  $\rho_*$  the polarization degree decreases as the star radius increases. We note that, similarly to limb-darkening measurements, the polarization degree is maximized for events with large finite source effects, namely for  $\rho_*/u_0 \simeq 1$ .

To compare the polarization degree for the three considered source models (hot, late type main sequence and cool giant stars), in Fig. 2 we show  $P$  versus  $\rho_*/u_0$ . As in Fig. 1, the maximum polarization occurs at  $\rho_*/u_0 \simeq 1$  and for low values of  $\rho_*$ . The polarization for late type stars is calculated in the I-band assuming  $q_I = 4.2 \times 10^{-4}$ ,  $k_I = 50$  and  $\Gamma_I = 0.5$ , that are typical parameter values for Sun like stars. As one can see the maximum polarization degree is in any case much lower than that for hot star sources. In the case of cool giant stars the polarization profile is not much different with respect to that for hot stars if  $\tau \simeq 10^{-3}$ . Of course, even larger values for  $P$  can be obtained, provided that  $\tau > 10^{-3}$ . In Fig. 2 we also see that there exists a limiting value of the ratio  $\rho_*/u_0$  ( $\simeq 1.7$  for  $\tau = 10^{-3}$ ) at which the polarization degree for cool giant stars overcomes that for hot stars. This is a relevant point since, as we shall see

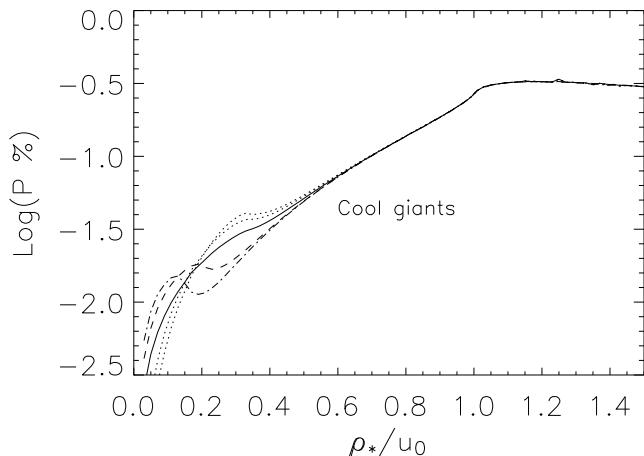


**Figure 3.** Polarization versus  $\rho_*/u_0$  in the case of cool giant stars. Assuming  $\tau = 10^{-3}$ , we show the effect of varying the model parameters. As a reference, the solid line corresponds to  $R_h = 3 R_*$  and  $\beta = 2$ . Dashed lines are for models with  $\beta = 2$  and increasing values of  $R_h = 5 R_*$  and  $R_h = 7 R_*$ . For these models a secondary polarization peak occurs at sequentially smaller values of  $\rho_*/u_0 < 1$ , as  $R_h$  increases. Dotted lines are for models with  $R_h = 3 R_*$  and increasing values of  $\beta = 3$  (bottom) and  $\beta = 4$  (upper).

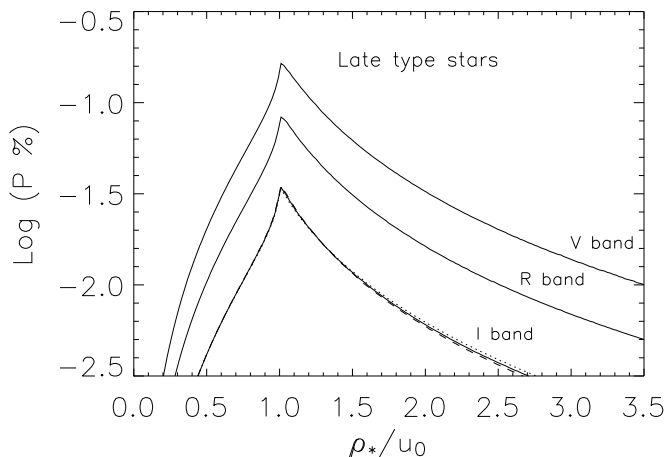


**Figure 4.** Polarization versus  $\rho_*/u_0$  for late type stars. Assuming  $\rho_* = 0.01$  and  $\Gamma = 0.5$ , we show the polarization versus  $\rho_*/u_0$  in the V, R, I band (solid lines). For the I band case the polarization is also shown for  $\Gamma = 0.1$  (dotted line) and  $0.9$  (dashed line).

later on, so large values of  $\rho_*/u_0$  are rather common in the microlensing events observed towards the Galactic bulge.

In Fig. 3 for cool giant stars we show how the polarization degree depends on the relevant model parameters (Simmons, Newsam & Willis 1995a; Simmons et al. 2002). We take  $\rho_* = 0.01$  and  $\tau = 10^{-3}$  and let the circumstellar envelope parameters  $\beta$  and  $R_h$  vary. For  $\rho_*/u_0 > 0.5$  the polarization degree is almost insensitive to the  $\beta$  and  $R_h$  values, since the polarization is mainly due to the source star disc.

In Fig. 4, for late type stars, we show how the polariza-

tion degree depends on the ratio  $\rho_*/u_0$  and the parameters  $\Gamma_\lambda$ ,  $q_\lambda$  and  $k_\lambda \equiv m_\lambda^{-1}$  in eqs. (11) and (12). To this aim, we consider the V, R, I bands for which, adopting the relations and the parameter values in Stenflo (2005), we obtain  $q_V = 2.5 \times 10^{-3}$ ,  $k_V = 18$  (in the V band),  $q_R = 1.2 \times 10^{-3}$ ,  $k_R = 23$  (in the R band),  $q_I = 4.2 \times 10^{-4}$ ,  $k_I = 50$  (in the I band). As one can see in Fig. 4 the polarization in late type stars is almost insensitive to variation of  $\Gamma$ , while it rapidly decreases from the V to I band. In this respect, polarization observations towards late type stars should be performed at low wavelength, at least for near enough objects for which absorption by interstellar medium is negligible. However, for polarization measurements towards Galactic bulge stars, the I band represents the best compromise between interstellar absorption and the dependence of the polarization on wavelength.

Concerning the polarization in exoplanetary events, as already mentioned, we find that one or more spikes appear in the polarization profiles when the caustics are crossed by the source star disc, corresponding to a large amplification of a narrow piece of the star surface. Outside the caustics, the polarization signal from the total stellar flux is almost vanishing. Clearly, in a real observation, the obtained polarization profile, in addition to the usual light-curve observations, may be used to constrain the binary system parameters.

To be more explicit on the expected polarization variability in microlensing, we now focus on a sample of highly magnified *transit* events (both single-lens and exoplanetary) observed towards the Galactic bulge by the OGLE and MOA collaborations (Choi et al. 2011). We also consider some *bypass* exoplanetary events towards the Galactic bulge for which the polarization signal is enhanced by the source star transiting a planetary caustics. The parameters of the best fit models to the light-curves are given for single-lens events in Table 1 and for exoplanetary events in Table 3.

### 3.1 Single-lens events towards the Galactic center

In Table 1 we give the parameters of 11 highly magnified single-lens events, selected among the 17 given in the Table 3 in Choi et al. (2011). The selected events are characterized by a clearly identified star source for which the physical parameters have been measured, also by follow up observations. Among them, 4 source stars are late type stars and 7 are cool giant stars. All events are characterized by very small values of their impact parameter ( $u_0 \ll 1$ ) and relatively large source size, so that  $\rho_*/u_0 > 1$ . In these events the lens crosses over the source star disc and therefore, at the peak of the event, different parts of the source are magnified by substantially different amounts. This fact provides a rare chance not only to measure the brightness profile of a remote star, as shown by Choi et al. (2011), but also to maximize the polarization effects.

#### 3.1.1 Late type main sequence source stars

Let us start by considering a subsample of the 4 events in Table 1 that consists of sources belonging to the population of late type main sequence stars (F and G spectral type). We evaluate the polarization profiles as a function of time by using in eqs. (1), (2) and (3) the polarization law

$P(\mu)$  in eq. (11), assuming the solar value for the parameters  $q_I = 4.2 \times 10^{-4}$  and  $k_I = 50$ . The adopted limb-darkening profile is given in eq. (12) where the values of the  $\Gamma_I$  coefficients are evaluated in the I band and given in Table 1. The polarization profiles of these 4 events, that are shown in Fig. 5, have a unique behavior characterized by the presence of a double peak that corresponds to the time instants at which the lens *enters* and *exits* the source star disc. The time interval between the two peaks, as calculated by eq. (17), is given in Table 2, where we also give the I band magnitude  $I_0$  at the instant  $t_0$  of maximum magnification. We note that, due to the typical small values of  $\Delta t_* \lesssim 1$  day, the source magnitude at the instant of maximum polarization is always very close to  $I_0$ . The maximum polarization value (occurring in correspondence of each peak) turns out to be  $\simeq 3 \times 10^{-2}$  percent, almost irrespective of the  $u_0$  and  $\rho_*$  values, since the ratio  $\rho_*/u_0 > 1$ . Indeed, the ratio  $\rho_*/u(t)$  is a function of time and always exists a time value  $t_{\max}$  at which  $\rho_*/u(t_{\max}) = 1.04$  where, as already shown, the polarization degree gets the maximum value. In between the two peaks the polarization profile depends on the ratio  $\rho_*/u_0$  (giving the extent of finite source effects) and rapidly flattens as  $\rho_*/u_0$  increases.

#### 3.1.2 Cool giant source stars

For the seven single-lens events in Table 1 whose source is a cool giant star, we calculate the polarization profile following the formalism of Subsection 2.4. For simplicity we fix the parameter values  $\beta = 2$  and  $R_h = 5R_*$ , irrespective of the source spectral type<sup>4</sup>. Of course, in this case the polarization degree depends on the optical depth  $\tau_I$  that is estimated from the  $\dot{M}$  value in eq. (16). It turns out that our sources are characterized by a stellar envelope with  $\tau_I$  in the range  $10^{-4} - 10^{-2}$ . The corresponding polarization curves are shown in Fig. 6. As for single-lens events with late type main sequence source stars (see Fig. 5), two polarization peaks are present (occurring when the lens enters and exits the source star disc) and the duration of the signal is related to the lensing parameters by eq. (17). We note in particular that the flat polarization profile in the case of the event OGLE-2011-BLG-1101/MOA-2011-BLG-325 is due to the large value of  $\Delta t_* \simeq 5$  day, which is larger of the time interval (3 days around  $t_0$ ) considered in the figure. In Table 2 we give for all the events the values of the magnitude  $I_0$  at the peak of the microlensing event, the time duration  $\Delta t_*$ , the optical depth  $\tau_I$  in the I band and the maximum value of polarization  $P_{\max}$ .

### 3.2 Exoplanetary events towards the Galactic center

Planetary perturbations on the single-lens magnification pattern are expected to fall in two classes. The first class of perturbations occurs when a source star passes near a planetary caustic. Although these perturbations are more common, they are also unpredictable and can occur at any

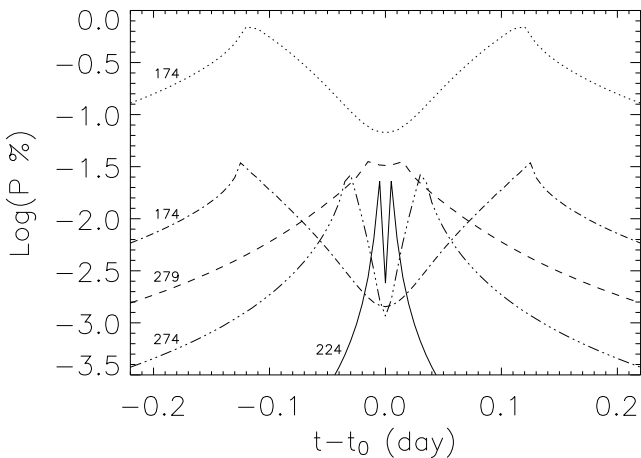
<sup>4</sup> As shown in Fig. 3, for  $\rho_*/u > 0.5$  and  $\rho_* < 0.01$ , the polarization degree is almost independent on the adopted parameter values, while it slightly depends on them otherwise.

**Table 1.** Parameters of 11 highly magnified single-lens events towards the Galactic bulge with identified source star type.

event	source type	$u_0$ ( $10^{-3}$ )	$t_E$ (day)	$\rho_*$ ( $10^{-3}$ )	Reference
OGLE-2007-BLG-224/MOA-2007-BLG-163	F V	0.29	6.91	0.9	Gould et al. (2009)
OGLE-2008-BLG-279/MOA-2008-BLG-225	G V	0.66	106.0	0.68	Yee et al. (2009)
MOA-2009-BLG-174	F V	0.5	64.99	2.0	Choi et al. (2012)
MOA-2011-BLG-274	G V	2.8	2.78	12.3	Choi et al. (2012)
OGLE-2004-BLG-254	K III	6.1	12.89	40.6	Cassan et al. (2006)/Choi et al. (2012)
OGLE-2004-BLG-482	M III	1	9.61	13.09	Zub et al. (2011)
MOA-2007-BLG-176	K III	36	8.09	59.4	Choi et al. (2012)
OGLE-2007-BLG-302/MOA-2007-BLG-233	G III	5.4	15.92	36.8	Choi et al. (2012)
OGLE-2008-BLG-290/MOA-2008-BLG-241	K III	2.76	16.36	22.0	Choi et al. (2012)
MOA-2011-BLG-093	G III	28.8	14.97	53.3	Choi et al. (2012)
OGLE-2011-BLG-1101/MOA-2011-BLG-325	K III	47.4	29.55	96.0	Choi et al. (2012)

**Table 2.** Calculated parameters for the same events in Table 1. Here  $I_0$  is the I band magnitude at  $t_0$  and  $P_{\max}$  is the maximum value of the polarization.

event	$I_0$ (mag)	$\Delta t_*$ (day)	$\rho_*/u_0$	$\Gamma_I$	$\tau_I$ ( $10^{-4}$ )	$P_{\max}$ (%)
OGLE-2007-BLG-224/MOA-2007-BLG-163	10.4	0.01	3.10	0.44	-	0.02
OGLE-2008-BLG-279/MOA-2008-BLG-225	12.6	0.03	1.03	0.52	-	0.04
MOA-2009-BLG-174	11.9	0.25	4	0.33	-	0.04
MOA-2011-BLG-274	13.3	0.07	4.39	0.52	-	0.03
OGLE-2004-BLG-254	12.0	1.03	6.65	-	7	0.23
OGLE-2004-BLG-482	11.4	0.25	13.09	-	6	0.20
MOA-2007-BLG-176	14.4	0.76	1.65	-	100	3.23
OGLE-2007-BLG-302/MOA-2007-BLG-233	11.9	1.16	6.81	-	35	1.14
OGLE-2008-BLG-290/MOA-2008-BLG-241	9.7	0.71	7.97	-	2	0.07
MOA-2011-BLG-093	12.2	1.34	1.85	-	5	0.16
OGLE-2011-BLG-1101/MOA-2011-BLG-325	11.9	4.93	2.03	-	20	0.65

**Figure 5.** Polarization profiles for highly magnified single-lens events, with late type source stars. For comparison purpose, assuming the same microlensing parameters of the MOA-2009-BLG-174 event, we show the polarization profile (dotted line) that one could expect in the case of a hot source star giving rise to a polarization à la Chandrasekhar.

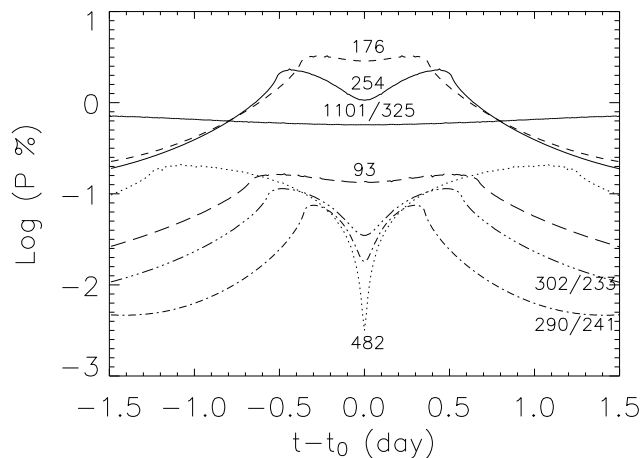
time during the event. The second class of planetary perturbations occurs in highly magnified events in which the source becomes very closely aligned with the primary central caustic. These events allow to probe the region of the central caustic (associated to the primary lens), that may be perturbed even by low-mass planets lying anywhere sufficiently close to the Einstein ring. Since in this case the time of occurrence of the event peak can be predicted in advance, it is possible to focus observing resources to make intensive observations around the peak of the event. This is, indeed, the strategy that has been adopted by the  $\mu$ -FUN collaboration (Gould et al. 2010) and that has allowed the discovery of half of the exoplanets detected by microlensing (Gaudi 2010). It goes without saying that this class of events may provide the highest chance to detect the polarization signals, at least for events showing large finite source effects, namely with  $\rho_*/u_0 > 1$ .

**Table 3.** Parameters of 6 exoplanetary events towards the Galactic bulge.

event	source type	$u_0$ ( $10^{-3}$ )	$q$ ( $10^{-3}$ )	$d$	$t_E$ (day)	$\alpha$ (deg)	$\rho_*$ ( $10^{-3}$ )	Reference
MOA-2007-BLG-400	LT/subgiant	0.25	2.6	0.34	14.41	227.06	3.26	Dong et al., 2009
MOA-2008-BLG-310	G V	0.27	2.5	2.87	14.43	226.99	3.29	Janczak et al., 2010
		3	0.331	1.085	11.14	69.33	4.93	
OGLE-2005-BLG-169	G V	3.01	0.32	0.927	11.08	69.33	4.95	Gould et al., 2006
		1.24	0.086	1.0198	42.27	117.00	0.44	
		1.25	0.083	0.9819	42.09	122.65	0.39	
OGLE-2005-BLG-390	K III	35.9	0.076	1.610	11.03	157.91	25.6	Beaulieu et al., 2006
OGLE-2003-BLG-235/MOA-BLG-53	G IV	133	3.9	1.120	61.5	223.8	0.96	Bond et al., 2004
MOA-2007-BLG-368	G V	82.5	0.127	0.9227	53.2	25.90	1.88	Sumi et al., 2010

**Table 4.** Calculated parameters for the events in Table 3.

event	$I_0$ (mag)	$\Delta t_*$ (day)	$\rho_*/u_0$	$\Gamma_I$	$\tau$ ( $10^{-4}$ )	$P_{\max}$ (%)
MOA-2007-BLG-400	9.9	0.10	13.04	0.47	-	0.02
MOA-2008-BLG-310	12.9	0.09	1.64	0.52	-	0.03
OGLE-2005-BLG-169	13.1	-	0.35	0.52	-	0.002
OGLE-2005-BLG-390	13.1	-	0.71	-	$10^{-3}$	0.10
OGLE-2003-BLG-235/MOA-BLG-53	17.6	-	0.007	0.52	-	0.01
MOA-2007-BLG-368	15.4	-	0.02	0.52	-	0.02


**Figure 6.** Polarization profiles for the 7 single lens events with giant source stars given in Table 2. For the event OGLE-2011-BLG-1101/MOA-2011-BLG-325 the maximum value of polarization ( $P_{\max} = 0.65$  percent) occurs at  $t - t_0 \simeq \pm 2.5$  days.

### 3.2.1 High magnification events

Up to now 15 exoplanets have been discovered by microlensing towards the Galactic bulge<sup>5</sup> in 14 systems. Among them, we consider in Table 3 six events representative of the two mentioned classes of planetary perturbations. Let

us start by considering the first 3 highly magnified exoplanetary events belonging to the first class, for which the source star passes near the primary lens. The events MOA-2007-BLG-400 (Dong et al. 2009) and MOA-2008-BLG-310 (Janczak et al. 2010) are *transit* events, while OGLE-2005-BLG-169 (Gould et al. 2006) is a *bypass* event. These events are characterized by late type (LT) source stars, even if the first source might be a subgiant star close to the turn off point. We calculate the expected polarization signal following Subsection 2.3, assuming  $q_I = 4.2 \times 10^{-4}$  and  $k_I = 50$  as for the Sun. The corresponding polarization profiles are shown in Fig. 7 (MOA-2007-BLG-400 and MOA-2008-BLG-310) and Fig. 8 (OGLE-2005-BLG-169).

As one can see, the polarization curves in Fig. 7 appear similar to those in Fig. 5 for single-lens events with source stars of the same nature, even if the presence of the planet in this case produces a little asymmetry with respect to  $t = t_0$ , that is not present in Fig. 5. This might offer in principle an independent test of the exoplanet presence from polarization measurements.

The third event in Table 3 is a highly magnified bypass event with a Neptune mass ratio  $q \simeq 8.6 \times 10^{-5}$  planetary companion to the primary lens star (Gould et al. 2006). This low mass planet is lying sufficiently close to the Einstein ring and so it is able to perturb the light-curve expected for a single-lens event. As one can see in Fig. 8, the polarization profile shows the presence of secondary peaks occurring when the star disc enters and exits the small central caustic associated with the planet and closely aligned with the host star. The features in the polarization curve closely resemble the residual pattern of the light-curve (see Fig. 1

<sup>5</sup> See <http://exoplanet.eu>.

in Gould et al. (2006)) and could be used in principle to independently constrain the binary system parameters. We would like to note that for this specific event the low value of the ratio  $\rho_*/u_0 = 0.38$  determines a rather low value of the polarization degree. An exoplanetary event with the same microlensing parameters but with larger finite size effects, should give a higher polarization degree potentially detectable.

### 3.2.2 Low magnification events

The last 3 events in the Table 3 are exoplanetary events of low magnification, in which the source star disc crosses a planetary caustic located far from host star, causing a peak in the polarization profile at  $t \neq t_0$ . The polarization is evaluated following the formalism in Section 2.3 and 2.4, depending on the nature of the source star.

In Fig. 9 for the event OGLE-2005-BLG-390 with a K giant source star, we use a value of  $\tau \simeq 10^{-3}$  which results from eqs. (15) and (16), once the measured source star parameter values (Beaulieu et al. 2006) are used. As one can see, the sharp peak in the polarization profile occurs at the same time ( $t \simeq 10$  day) of the planetary perturbation present in the light-curve (Fig. 1 in Beaulieu et al. (2006)). However, the relative increase of the polarization signal (with respect to the expectation for the single-lens model) is by far larger than the corresponding one in the light curve. We also note that the polarization peak shows a two subpeak structure caused by the source star disc transiting the planetary caustic. The size of this caustic, which turns out to be  $\lesssim \rho_*$ , may be computed by using the eqs. (8) and (9) given by Han (2006). The sharp depolarization following the polarization peak in Fig. 9 is due to a deamplification region (following the planetary caustic) intersected by the source star disc.

The polarization profile evaluated for the exoplanetary event OGLE-2003-BLG-235/MOA-BLG-53 (Bond et al. 2004) is shown in Fig. 10, where we follow the approach described in Subsection 2.3 for late type main sequence stars. As one can see the polarization degree is almost vanishing, except for two sharp peaks, also present in the light-curve (see Fig. 1 in Bond et al. (2004)), occurring when the source passes over two folds of the planetary caustic. The size of this caustic is much larger than the projected source star disk, which enters the caustic at  $t \simeq -13$  day and exits at  $t \simeq -6$  day.

A similar behavior occurs for the last considered exoplanetary event MOA-2007-BLG-368 (Sumi et al. 2010) as shown in Fig. 11.

### 3.3 Polarization profile for the PA-99-N2 event towards M31

The PA-99-N2 event is a pixel lensing event observed in 1999 towards M31 by the Point-Agape Collaboration (Paulin-Henriksson et al. 2003). The light curve shows a deviation from the Paczyński law which has been thoroughly analyzed by An et al. (2004). In particular, An et al. (2004) concluded in favor of a binary lens system with the primary lens companion being in the substellar mass range. A further Monte Carlo study (Ingresso et al. 2009, 2010) has evidenced that one of the binary component may even be

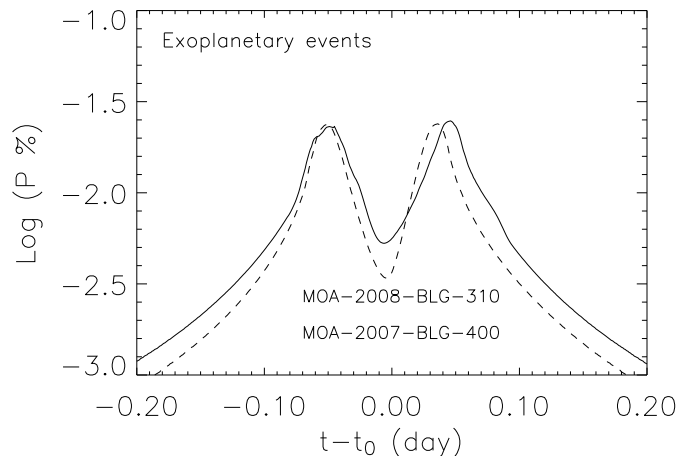


**Figure 7.** Polarization profiles for the exoplanetary events MOA-2008-BLG-310 (solid line) and MOA-2007-BLG-400 (dashed line). In both cases the lens system transits the source star and the polarization is calculated for the late type source star case.

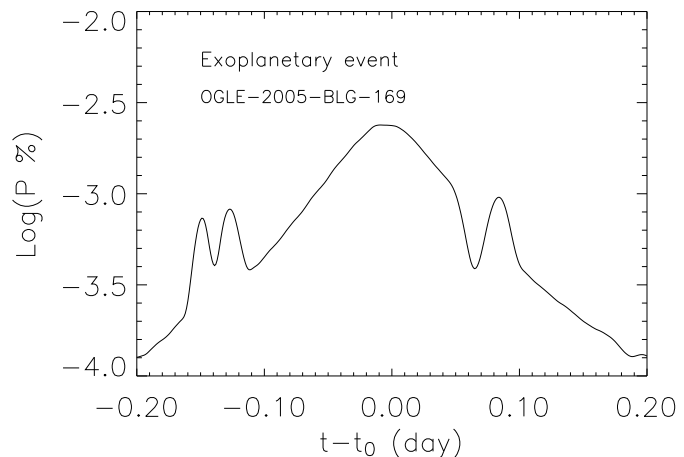


**Figure 8.** Polarization profile for the exoplanetary event OGLE-2005-BLG-169. The lens bypasses the source star.

an exoplanet of a few Jupiter masses. Although the analysis of An et al. (2004) does not provide a strong evidence for finite size source effect, which is necessary to the enhancement of the polarization signal, to our purposes we consider the lensing parameter for the binary finite source (FS) solution provided in Table 2 in the paper by An et al. (2004). In particular, for the source we consider a red giant with  $R \simeq 85 R_\odot$  and  $T_{\text{eff}} \simeq 3700$  K. Accordingly, from eqs. (15) and (16) we estimate  $\tau \simeq 10^{-2}$  and using the formalism in Subsection 2.4 we compute<sup>6</sup> the corresponding polarization profile shown in Fig. 12. Inspection of this figure shows that

<sup>6</sup> We note that the polarization  $P$  has been always calculated by considering only the flux  $F$  from the lensed source star and neglecting any contribution of non-lensed sources (blending). In this respect, our polarization results for the PA-99-N2 event have to be considered as upper limits, since a strong blending component is expected in pixel-lensing observations towards M31.

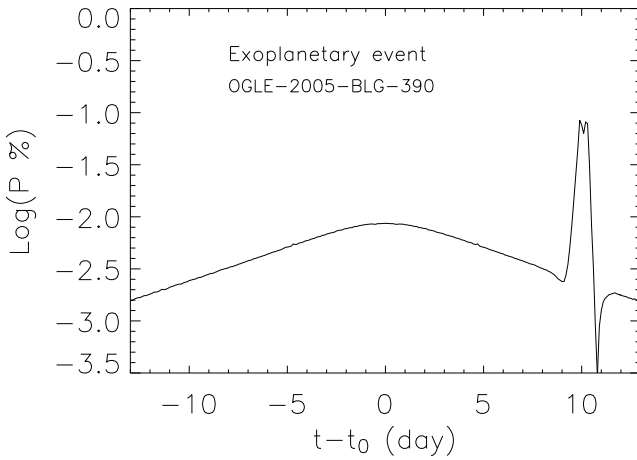


**Figure 9.** Polarization profile for the exoplanetary event OGLE-2005-BLG-390.

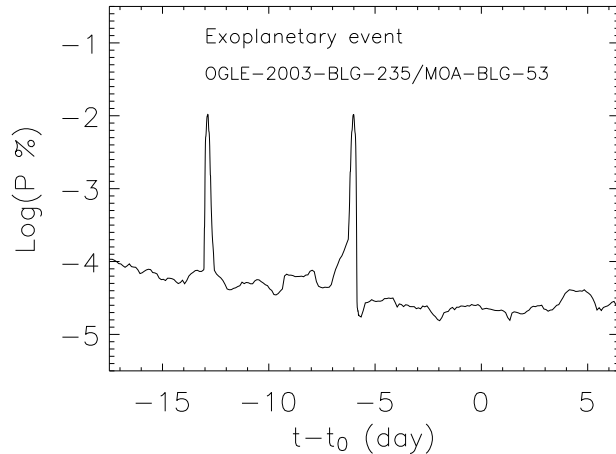


**Figure 10.** Polarization profile for the exoplanetary event OGLE-2003-BLG-235/MOA-BLG-53.

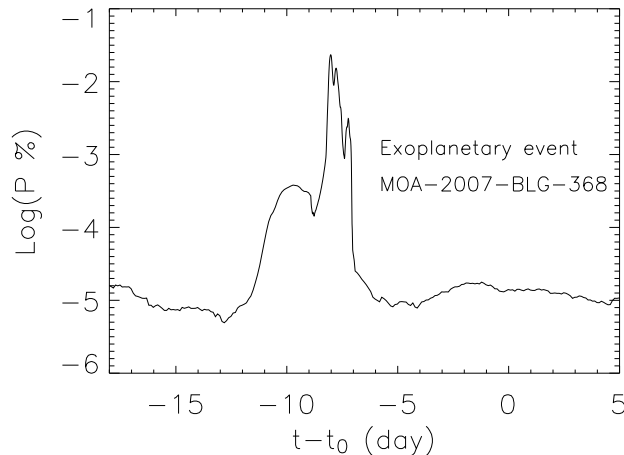


**Figure 11.** Polarization profile for the exoplanetary event MOA-2007-BLG-368.

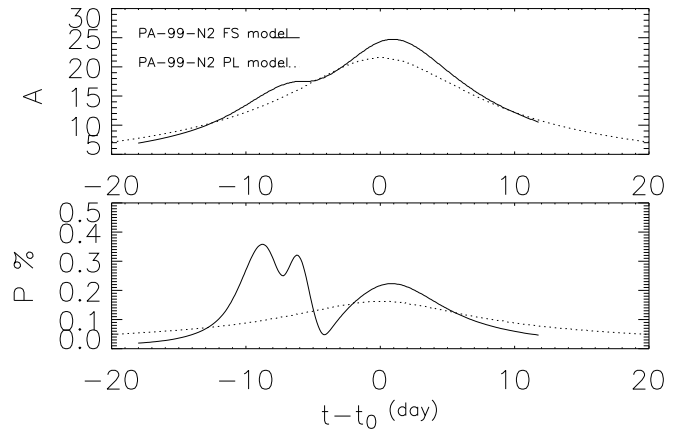


**Figure 12.** Magnification (upper panel) and polarization profiles (lower panel) for the event PA-99-N2 towards M31. Solid (dotted) lines are used for the FS (PL) model in Table 2 in An et al. (2004).

the amplitude of the polarization degree can reach values up to 0.5 percent (when the caustic region is crossed by the source star). In the same figure, for comparison, we show the polarization curve (dotted line) expected for a point lens (PL) model with the same finite source effect.

Of course, with a distance modulus to M31 larger by about 10 mag than that of Galactic bulge stars, the observability of the polarization for M31 sources remains, at the moment, highly speculative.

#### 4 DISCUSSION AND CONCLUSIONS

The combined effects of large magnification and finite size source effects in some microlensing events may allow to get relatively large values of the polarization of the light from the source stars. In this paper we calculate the polarization profile as a function of the time for a selected sample of both single and exoplanetary microlensing events observed towards the Galactic bulge, by taking into account the nature of the source star: hot, late type main sequence and cool giant stars. Indeed, different polarization mechanisms take place in the stellar atmospheres, depending on the source star type: photon (Thomson) scattering on free electrons, coherent (Rayleigh) scattering off atoms and molecules, and photon scattering on dust grains, for hot, late type and cool giant stars (with extended atmospheres), respectively.

The analysis of the polarization curves for single-lens, highly magnified microlensing events towards the Galactic bulge has shown that the polarization degree of the stellar light can reach values as high as 0.04 percent at the peak in the case of late type source stars and up to a few percent in the case of cool giant source stars (red giants) with extended envelopes. For these events the primary lens crosses the source star disc (*transit* events) and relatively large values of  $P$  are thereby produced due to large finite source effects and the large magnification gradient throughout the source star disc. The time duration of the peak of the polarization signal may vary, from 1h to 1day, depending on the source star radius and the lens impact parameter.

Similar values of polarization may also be obtained in exoplanetary events when the source star crosses the primary or the planetary caustics. While in the former case (as for single-lens events) the peak of the polarization signal always occurs at symmetrical points with respect to the instant  $t_0$  of maximum magnification, in the latter case the polarization signal may occur at any (and generally unpredictable) time during the event.

The natural question which arises is whether such polarization signals may be detectable with the present or near future technology. Polarimeters are nowadays available on large telescopes and the best possibility for measuring polarization in the R and I bands is offered at present by the polarimeter in FORS2 on ESO's VLT telescope. With this instrument it is possible to measure the polarization for a 12 mag source star with a precision of 0.1 percent in 10 min integration time, and for a 14 mag star in a 1h. Indeed, for a few of the events considered in Tables 2 and 4 the peak  $I_0$  magnitude is  $\simeq 12$  with the expected maximum polarization degree lasting up to 1 day, thus suggesting that polarization measurements in highly magnified microlensing events constitute a realistic target of opportunity for currently available instruments.

It goes without saying that polarization measurements in microlensing events require an alert system able to predict in advance the instant of the occurrence of the polarization peak. A alert system is already in operation based on OGLE and MOA survey data <sup>7</sup>, and it is particularly efficient in the case of highly magnified events, allowing to focus observing resources to make intensive observations around the peak of the event.

We emphasize that polarization measurements in highly magnified microlensing events offer an unique opportunity to probe stellar atmospheres of Galactic bulge stars. Besides the interest related to stellar astrophysics, the analysis of the polarization profile, which reflects that of the magnification light-curve, given sufficient observational precision, may in principle provide independent constraints on the lensing parameters also for exoplanetary events.

## ACKNOWLEDGMENTS

We thank the referee, R. Ignace, for useful comments and suggestions. We also thank H. M. Schmid and R. Gratton for useful discussions. SCN thanks the Swiss National Science Foundation for support during this work.

## REFERENCES

- Agol, E., 1996, MNRAS, 279, 571.  
 Alcock, C., Akerloff, C. W., Allsman, R. A., et al., 1993, Nature, 365, 621.  
 Alcock, C., Allen, W. H., Allsman, R. A. et al., 1997, ApJ, 491, 436.  
 An J. H., Evans N. W., Kerins E. et al., 2004, ApJ, 601, 845.  
 Aubourg, E., Bareyre, P., Brehin, S., et al., 1993, Nature, 365, 623.  
 Beaulieu, J.-P., Bennett, D. P., Fouqu e, P. et al. 2006, Nature 439, 437.  
 Belokurov, V. A. & Sazhin M. V., 1998, Phys. Lett. A 239, 215.  
 Bochkarev, N. G., Karitskaya, E. A., 1983, Soviet Astron. Lett. 9, 6.  
 Bochkarev, N. G., Karitskaya, E. A., & Sakhbullin, N. A. 1985, Ap & SS 108, 15.  
 Bogdanov, M. B. & Cherepashchuk, A. M., 1995a, Astron. Lett. 21, 505.  
 Bogdanov, M. B. & Cherepashchuk, A. M., 1995b, Astron. Rep. 39, 779.  
 Bogdanov, M. B. & Cherepashchuk, A. M., Sazhin, M. V. 1996, Ap&SS 235, 219.  
 Bogdanov, M. B. & Cherepashchuk, A. M., 2000, Astron. Rep. 44, 745.  
 Bogdanov, M. B. & Cherepashchuk, A. M., 2002, Astron. Rep. 46, 996.  
 Bond, I. A., Udalski, A., Jaroszyski, M., et al., 2004, ApJ 606, L155.  
 Calchi Novati, S., Gen. Rel. Grav., 2010, 42, 2101.  
 Carciofi, A. C. & Magalhaes, A. M., 2005, ApJ 635, 570.  
 Cassan, A., Beaulieu, J.-P., Fouqu e, P. et al., 2006, A&A, 460, 277.  
 Chandrasekhar, S., 1950, Radiative Transfer, (Oxford, Clarendon Press).  
 Choi, J.-Y., Shin, I.-G., Park, S.-Y. et al., 2012, ApJ 751, 41.  
 Claret, A., 2000, A&A, 363, 1081.  
 Dolginov A. Z., Gnedin Yu. N., Silant'ev N. A., 1995, Propagation and Polarization of Radiation in Cosmic. Media, (New York, Gordon and Breach).  
 Dominik, M., 2005, MNRAS 361, 300.  
 Dominik, M., 2010, Gen. Rel. Grav., 42, 2075.  
 Dong S., Dong, S., Bond, I. A. et al., 2009, ApJ 698, 1826.  
 Einstein, A., 1936, Science, 84, 506.  
 Ferguson, J. W. at al., 2005, ApJ 623, 585.  
 Flury, D. M. & Stenflo, J. O., 1999, A&A 341, 902.  
 Fouqu e, P., Heyrovsk y D., Dong, S., 2010, A&A 518, A51.  
 Gaudi, B. S. & Gould, A., 1999, ApJ, 513, 619.  
 Gaudi, B. S., 2010, Refereed chapter in EXOPLANETS, edited by S. Seager, Tucson, AZ: University of Arizona Press, p. 79.  
 Gould, A., 1994, ApJ, 421, L71.  
 Gould, A., Udalski, A., An, D. et al., 2006, ApJ, 644, L37.  
 Gould, A., Udalski, A., Monard, B, et al., 2009, ApJ, 698, L147.  
 Gould, A., Dong, S.; Gaudi, B. S. et al., 2010, ApJ, 720, 1073.  
 Gurevich, A. V. & Zybin, K. P., 1995, Phys. Lett. A, 208, 276.  
 Han, C., 2006, ApJ, 638, 1080.  
 Hendry, M. A., Coleman, I. J., Gray, N., Newsam, A. M. & Simmons, J. F. L., 1998, New Astr. Rev., 42, 125.  
 Heyrovsk y D. & Sasselov, R. D., 2000, ApJ, 529, 69.  
 Heyrovsk y D., 2003, ApJ, 594, 646.  
 Heyrovsk y D., 2007, ApJ, 656, 483.  
 Ignace, R., Bjorkman, E. & Bryce, H. M., 2006, MNRAS, 366, 92.  
 Ignace, R., Bjorkman, E. & Bunker, C., 2008, in Pro-

<sup>7</sup> www.OGLE.astrouw.edu.pl  
 www.phys.canterbury.ac.nz/MOA

- ceedings of the Manchester Microlensing Conference: The 12th International Conference and ANGLES Microlensing Workshop, eds. E. Kerins, S. Mao, N. Rattenbury and L. Wyrzykowski, PoS(GMC8)002.
- Ingrosso, G., Calchi Novati, S., de Paolis, F. et al., 2006, *A&A* 445, 375.
- Ingrosso, G., Calchi Novati, S., de Paolis, F. et al., 2009, *MNRAS* 399, 219.
- Ingrosso, G., Calchi Novati, S., de Paolis, F. et al., 2011 *Gen. Rel. Grav.*, 2011, 43, 1047.
- Kayser, R., Refsdal, S. & Stabell, R., 1986, *A&A*, 166, 36.
- Janczak, J., Fukui, A., Dong, S. et al., 2010, *ApJ* 711, 731.
- Loeb, A. & Sasselov, D., 1995, *ApJ* 449, L33.
- Paczynski, B., 1986, *ApJ*, 304, 1.
- Paulin-Henriksson, S., Baillon, P., Bouquet, A. et al. 2003, *A & A*, 405, 15.
- Simmons, J. F. L., Newsam, A. M. & Willis J. P., 1995, *MNRAS*, 276, 182.
- Simmons, J. F. L., Willis J. P., Newsam, A. M., 1995, *AA*, 293, L46.
- Simmons J. F. L., Bjorkman J. E., Ignace R., Coleman I. J., 2002, *MNRAS*, 336, 501.
- Schneider, P. & Wagoner, R. V., 1997, *ApJ*, 314, 154.
- Schneider, P., Ehlers, J. & Falco E. E., 1992, *Gravitational Lensing*, Springer, Berlin.
- Schneider, P., & Weiss, A., 1992, *A & A*, 260, 1.
- Sobolev, V. V., 1949, *Uchen Zap. LGU, Ser. Math.* 16, 1 (Scientific Reports of Leningrad University).
- Sobolev, V. V., 1963, *A Treatise of Radiative Transfer*, (Toronto, Van Scientific Reports of Leningrad University).
- Stenflo, J. O., 2005, *A&A* 429, 713.
- Sumi T., Bennett, D. P., Bond, I. A. et al., 2010, *ApJ* 710, 1641.
- Suzuki, T. K., 2007, *ApJ* 659, 1592.
- Udalski, A., Szymański, M., Katożny, J. et al. 1993, *Acta Astronomica*, 43, 289.
- Udalski, A., Szymański, M., Katożny, J. et al. 1994, *ApJ*, 426, L69.
- Valls-Gabaud, D., 1998, *MNRAS*, 294, 747.
- Wambsganss, J., 1997, *MNRAS*, 284, 172.
- Witt, H. J., & Mao, S., 1994, *ApJ*, 430, 505.
- Witt, H. J., & Mao, S., 1995, *ApJ*, 447, L105.
- Yee, J. C., Udalski, A., Sumi, T. et al., 2009, *ApJ*, 703, 2082.
- Yoshida, H., 2006, *MNRAS* 369, 997.
- Zakharov, A. F. 1995, *A & A* 293, 1.
- Zakharov A. F. & Sazhin, M. V. 1996a, *J. Exper. Theor. Phys.*, 83, 1057.
- Zakharov A. F. & Sazhin, M. V. 1996b, *J. Exper. Theor. Phys. Lett.* 63, 937.
- Zakharov, A. F. 1998, *Phys. Lett. A & A* 250, 67.
- Zakharov, A. F. 1999, *Astron. Rep.* 43, 325.
- Zakharov, A. F. 2010, *Gen. Rel. Grav.* 42, 2301.
- Zub, M., Cassan, A., Heyrovský, D. et al., 2011, *A&A*, 525, A15.